Recrystallization Rates and Processes in Laser-Amorphized Poly(ethylene terephthalate)

Philip D. Richards and Eric Weitz*

Department of Chemistry, Northwestern University, Evanston, Illinois 60208

A. J. Ouderkirk* and D. S. Dunn

3M Corporation, CRPTL, St. Paul, Minnesota 55144

Received October 6, 1992; Revised Manuscript Received November 30, 1992

ABSTRACT: The recrystallization of laser-amorphized poly(ethylene terephthalate) (PET) films has been followed in real time using infrared spectroscopy. The laser amorphization process produces a unique set of conditions which makes possible a simplified interpretation of the data obtained during recrystallization of thin films. The observed data for the time dependence of the growth of recrystallized PET fits well to a kinetic model which includes both primary and secondary crystallization processes. Values obtained for the rate of the primary process agree well with literature values for spherulitic growth in PET, reaching a maximum rate of 94 nm/s at 170 °C. The nature of the primary and secondary processes is discussed.

I. Introduction

Polymer crystallization kinetics are typically studied by measuring the fraction of crystallized material as a function of time at a particular temperature.[1-4] Interpretation of these experimental data involving measurements of the degree of crystallinity in a bulk sample in terms of rates and mechanisms of crystallization is complicated by the fact that nucleation is normally a random process. For example, optical microscopy directly measures the rate of growth of the crystallization front but does not provide any details on secondary processes that may further increase the order of the polymer.

Pulsed UV excimer lasers have recently been used to amorphize the surface of semicrystalline polymers.[5] This process uses a short pulse of UV light to heat the surface of a polymer above its melting point. The resulting material is an amorphous layer with a thickness of 30–100 nm on an unmodified base of the same polymer. The combination of a planar amorphous layer in direct contact with the nucleating surface of the unmodified semicrystalline base provides a unique opportunity to study the kinetics and mechanism of polymer crystallization. Prior studies imply that the chemical structure of the laser-amorphized polymer is unchanged during the brief melt–quench cycle.[5]

IR spectroscopy is a sensitive probe of the conformational order of a polymeric system.[6,7] In principle, the time-resolved spectra of a crystallizing system can fully characterize not only primary crystallization but possible secondary effects as well. To obtain maximal information regarding a system, the IR beam must probe a volume of polymer with a well-defined crystallization history. Ideally, the time of initiation of crystallization is well known and the sample is free from polymer with significantly different crystallization history. Laser amorphization provides an unambiguous definition of the start of the crystallization process in addition to well-defined crystallization growth.

As indicated above, laser heating of a polymer surface creates a thin layer of amorphous polymer on an underlayer of semicrystalline material. In other studies, IR techniques have been used to show that the degree of amorphization is complete through a depth of 30–100 nm, followed by a 0–20-nm transition zone between the amorphous layer and the semicrystalline base.[5,8] Thus, in principle, the rate of recrystallization as a function of temperature can be measured by amorphizing part of a polymer film using a laser pulse to initiate rapid melting and following subsequent recrystallization via infrared spectroscopy.

We have developed a system that uses rapid-scan FTIR spectroscopy to follow IR band intensities of vibrational modes in polymer films. Since the crystalline and amorphous states of polymers typically exhibit differences in IR positions and/or intensities, this system can monitor the degree of crystallization of a polymer in real time and produce spectra that potentially provide direct information on crystallization rates and mechanisms.

II. Experimental Section

Sample films of PET (number-average MW of 27 000) were spin cast from *o*-chlorophenol solution onto gold-coated polished silicon wafers. Solution preparation was done in air. The amorphous spin-cast films were then dried in a vacuum oven at 75 °C for 2 h. Semicrystalline films were prepared through thermal crystallization of amorphous films at 200 °C for 2 h under vacuum. Film thicknesses were measured by ellipsometry to be approximately 150 nm.

Infrared spectra were acquired using an infrared reflection absorption spectroscopy (IRRAS) configuration.[9] Previous studies have shown that there is an enhancement in the electric field of infrared radiation when it is incident upon a highly reflective surface at a glancing angle.[10] The IRRAS technique utilizes this phenomenon and thereby allows spectra of very thin films to be obtained. In this geometry the IR beam from the interferometer is incident on the sample at an angle of 78° relative to the surface normal. The film substrate serves as a mirror to reflect the IR beam onto a HgCdTe detector. This is shown schematically in Figure 1.

Measurements were made using a Nicolet 60SX spectrometer. The spectrometer was capable of making time-resolved measurements using rapid-scan software. In this mode interferograms are collected on each mirror pass and consecutively saved in memory for additional processing. For the present experiments spectra were collected at 29-ms intervals with a spectral resolution of 10 cm^{-1}. A pulse generated by the spectrometer on initiation of the rapid-scan cycle was appropriately delayed and used to trigger an excimer laser used to heat the PET film.

A Lambda Physik 201 MSC laser operating on KrF at 248 nm at 12–15 mJ/cm^2 was used to treat the sample films which were kept under a nitrogen purge within the sample compartment of the spectrometer. For temperature-dependent measurements, the thin films were supported in the sample compartment by an iron block heated by a circulating hot oil bath. Recrystallization was studied over a temperature range of 120–220 °C.

0024-9297/93/2226-1254$04.00/0

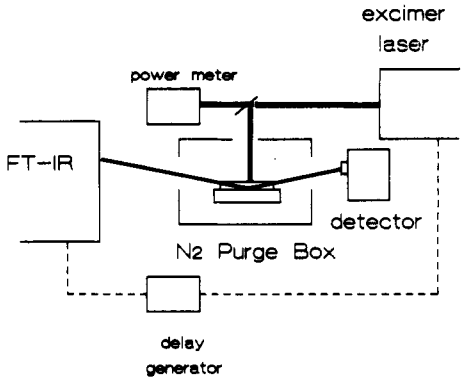

Figure 1. Time-resolved FTIR apparatus. An excimer laser used for treatment of the sample is triggered by a delayed pulse from the spectrometer generated on initiation of the rapid-scan sequence. The infrared radiation is incident on the sample in an IRRAS configuration within a nitrogen-purged sample chamber.

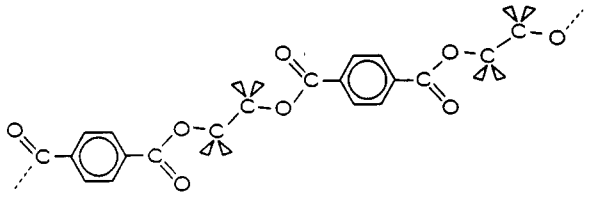

Figure 2. Structure of poly(ethylene terephthalate). Two repeating units are shown.

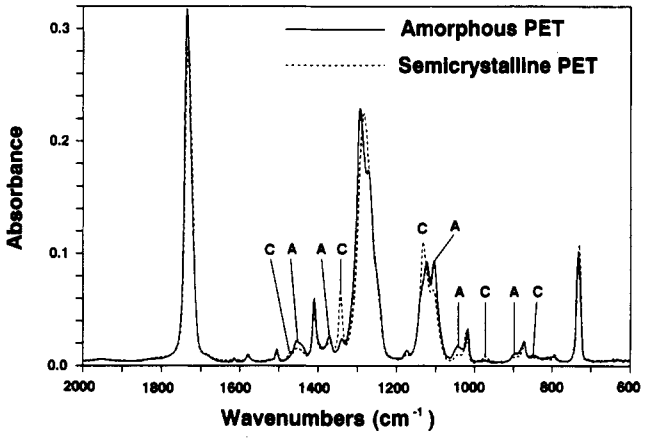

Figure 3. Infrared reflection absorption spectra of amorphous and semicrystalline PET thin films. A indicates absorption bands characteristic of amorphous PET, and C indicates absorption bands characteristic of semicrystalline PET.

III. Results

A. Data. PET is a well-studied polymer with an equilibrium melting temperature that has been reported between 271 and 300 °C and a glass transition temperature of 67 °C.[11] The structure of PET is shown in Figure 2. As shown in Figure 3, PET exhibits significant differences between the infrared spectra of the amorphous and crystalline states. In the crystalline state IR data indicate a trans configuration about the ethylene glycol fragment.[6,7] This configuration is also consistent with X-ray data which indicate a planar structure for PET.[12] The amorphous state however has been seen to have a gauche configuration and a loss of planarity.[6,7]

Changes in the IR spectrum of PET films were monitored during the recrystallization process. Recrystallization rates could in principle by determined by monitoring either the decay of amorphous bands or the recovery of semicrystalline bands. The crystalline-sensitive band at 1340 cm^{-1}, assigned to a CH_2 wagging mode of the ethylene glycol linkage, showed a significant change on amorphization and was used to generate the rate data presented here. A spectrum of the sample prior to laser treatment was used as a background for spectra collected during recrystallization. Thus bands indicative of the amorphous state are seen as positive absorptions and bands associated with the depleted semicrystalline material are seen as "negative" absorptions.

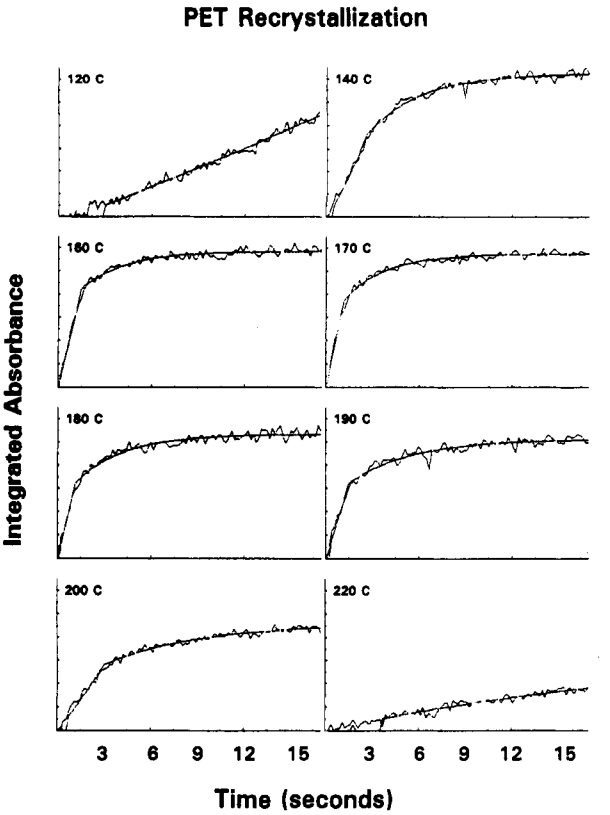

Figure 4. Experimental data showing the relative integrated absorbance of the semicrystalline sensitive band at 1340 cm^{-1} as a function of time for several different recrystallization temperatures. Fits of the data to eq 2 are shown with the data.

The rate of recrystallization in the films was monitored by observing changes in the intensity of the 1340-cm^{-1} crystalline-sensitive band as a function of time. Several such plots of the integrated peak area from 1366 to 1328 cm^{-1} are shown in Figure 4 for various recrystallization temperatures. The data in Figure 4 indicate that for the temperature extremes crystallization was not complete on the time scale of the measurements, whereas the intermediate temperatures showed little change in degree of crystallinity after the first few seconds. This behavior is consistent with the reported temperature dependence of PET crystallization rates.[11]

B. Model. To compare the data presented here for the rate of change of the fraction in the crystalline state to known linear growth rates obtained from studies of spherulitic growth, a knowledge of the manner in which the polymer crystallizes is necessary. The most common model used to describe polymer crystallization and to report data on crystallization kinetics is the Avrami model.[1-4] In this model the fraction of material crystallized varies as a function of time according to eq 1. In this

$$X_c = 1 - \exp(-kt^n) \quad (1)$$

equation k contains rate parameters for nucleation and growth and n is a parameter which can be indicative of the nucleation mechanism and the number of dimensions in which crystallization proceeds. This model was derived

Scheme I

$$A \xrightarrow{k_1} B \xrightarrow{k_2} C$$

$t < t_s$	$t > t_s$
$dA/dt = -k_1$	$A = 0$
$dB/dt = k_1 - k_2B$	$dB/dt = -k_2B$
$dC/dt = k_2B$	$dC/dt = k_2B$
$A(t) = A_0 - k_1t$	$A(t) = 0$
$B(t) = (k_1/k_2)(1 - e^{-k_2t})$	$B(t) = B(t_s)(e^{-k_2(t-t_s)})$
$C(t) = k_1(t - (1/k_2)(1 - e^{-k_2t}))$	$C(t) = B(t_s)(1 - e^{-k_2(t-t_s)}) + C(t_s)$

assuming a uniform distribution of nucleation sites with growth proceeding from these sites in random directions. The unique preparation and treatment of these samples result in a situation where neither of these assumptions is valid and thus a new model is needed.

The manner in which PET crystallizes under our experimental conditions has been determined independently of the rate data presented here via a depth-profiling technique and is described in more detail elsewhere.[13] Briefly, what is observed is a crystallization front nucleated by the interface between amorphized and untreated material which propagates perpendicular to the interface. The thickness of the transition region which represents the recrystallization front is small with respect to the amorphization depth produced by the initial laser-induced melting process. Once this initial crystallization front has transformed the material, there is also the possibility of one or more secondary processes which further increase the degree of crystallinity. The existence of secondry recrystallization processes has been the subject of much speculation,[1,2] and the observation of such processes has been recently reported by a few groups.[14,15] Though the exact nature of these processes is not known, they are likely to involve a further minimization of energy of the polymer chains, possibly by rearrangement and/or rotations of the various polymer subunits within crystalline regions of the polymer. A model in which the recrystallization process involves more than a single step is supported by the fact that the data in Figure 4 cannot be fit well to a simple functional form such as that expected for a simple first-order or bimolecular process (see section III.C). Given the observations discussed above, the kinetic mechanism shown in Scheme I was developed to describe the data in Figure 4.

The transformation is described as an A to B to C process, where A is the population of the amorphous state, B is the population of the primary crystalline material, and C is the population of the secondary crystalline material. The A to B step involves a crystallization front moving at a constant velocity through the polymer film. The recrystallization front has a finite thickness which is directly related to the thickness of the original transition region, but since the thickness of the front is small in comparison to the depth of the amorphized region, it has been neglected and in the model discussed above the recrystallization front has been treated as a plane. At times before this primary crystallization front has reached the surface of the film, $t < t_s$, the population of amorphous material is predicted to decay with time by a zero-order process as the recrystallization front moves through the film at a constant linear rate. The primary crystal is formed by this constant-rate primary process and also depleted by the secondary crystallization process which is first order in the population of B. Finally, C is produced by the secondary process, which is first order in the population of B. For times after the primary crystallization front has reached the surface, $t > t_s$, all of the amorphous material has been transformed by the primary process and thus the population of A is 0. At time greater than t_s, B is no longer being produced by the primary process and thus the populations of B and C are controlled by the transformation of B to C. This then gives exponential behavior for the populations of B and C with a time origin of t_s.

Table I

temp (°C)	$k_1(t_s)^a$	k_1(fit)^a	$k_2{}^b$
120	<5	<5	
140	37	37	0.29
160	73	73	0.34
170	94	94	0.38
180	92	91	0.32
190	78	78	0.24
200	35	37	0.16
220	<7	<7	

[a] Values for k_1 (in Scheme I) are in units of nm/s. $k_1(t_s)$ was calculated from the amorphization thickness divided by t_s. k_1(fit) was obtained from the least squares fit of the data and converted into units of nm/s by multiplying by the amorphization thickness. [b] In units of s^{-1}.

C. Fits. The data were fit to eq 2 using the simplex algorithm for a nonlinear least squares fit.[16] In equation

$$X_c(t) = ((\text{abs } B)\ B(t)) + ((\text{abs } C)\ C(t)) \qquad (2)$$

2, $B(t)$ and $C(t)$ are the time-dependent populations of B and C as given in Scheme I and (abs B) and (abs C) are the relative absorption coefficients of B and C. The relative absorbance of C was defined to be the asymptotic level reached in the plots of fraction recrystallized as a function of time. Thus the three parameters k_1, k_2, and the relative absorbance of B were fit by the program for a given value of t_s. Such fits were obtained for multiple values of t_s until a minimum in the error of the fits was achieved. Thus the value of t_s which gives the best fit to eq 2 corresponds to the time at which the primary crystallization front reaches the surface. Given this model of recrystallization, the linear crystallization rate can then be obtained simply by dividing the original thickness of the laser-amorphized layer by the time that is required for the primary crystallization front to reach the surface. As expected, the rates for primary recrystallization obtained in this manner agree extremely well with the values for k_1 obtained from fits to eq 2. These rates are presented in Table I. A comparison of the residual of the fit of eq 2 to the data at 170 °C to the residual from a single-exponential fit is shown in Figure 5. Attempts to fit the data to a single bimolecular functionality were also not successful.

IV. Discussion

A. Comparison to Previous Data. There have been numerous previous reports of crystallization kinetics for PET.[1] The majority of techniques used were only sensitive to the overall degree of crystallinity in the samples, making it difficult to differentiate secondary crystallization processes from primary processes. Most also studied samples undergoing random thermal nucleation. Because of these complications and the lack of direct knowledge of crystallization mechanisms, it has been difficult to relate the rate parameters for bulk crystallization obtained in these prior studies to the linear growth rate of the crystal. Direct measurements of linear growth rates have been made in studies of spherulitic growth by optical microscopy and light scattering techniques.[1,17] Since these methods directly measure the size of growing crystallites, they are only sensitive to primary crystallization. The data ob-

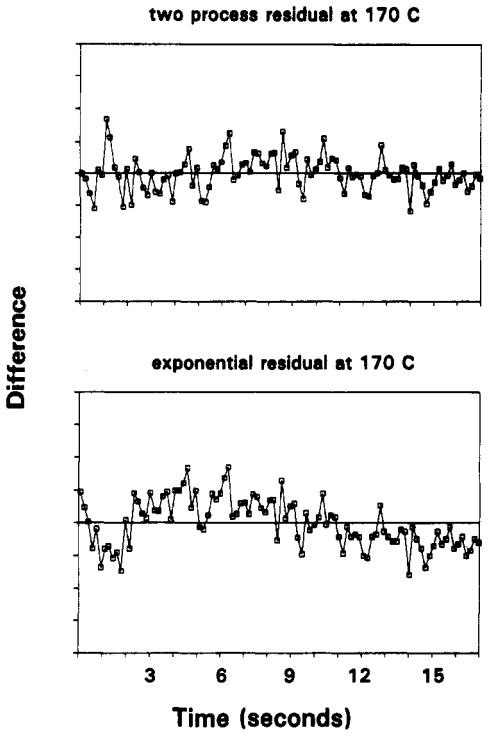

Figure 5. Residuals from the fits of the data obtained at 170 °C to a single exponential and to eq 2.

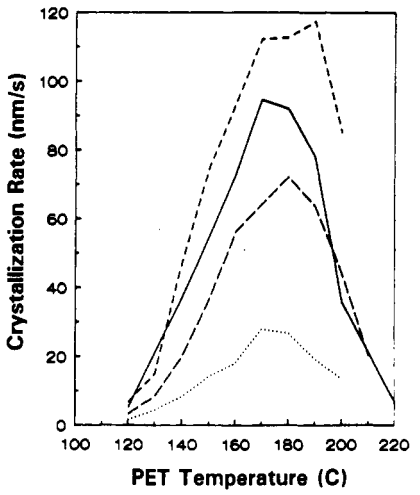

Figure 6. Comparison of the primary crystallization rate as a function of temperature obtained in this work with literature values from ref 12 for the temperature-dependent spherulitic growth rate for PET at several different molecular weights. Our data (—); MW = 19 000 (- - -); MW = 27 400 (– – –); MW = 39 100 (···).

tained by these methods are then comparable to our measured rates for primary crystallization. In Figure 6 the rate data obtained for the primary process are shown with previously reported linear growth rates for several different molecular weights of PET.[11] It can be seen that there is good agreement between the rate seen for our samples (MW 27 000) and the previously reported rates for samples with a molecular weight of 27 400. This agreement also implies that the laser treatment process causes no significant change in the chemical nature of the sample.

B. Possible Additional Recrystallization Mechanisms. It is useful to consider if it is necessary to include additional crystallization mechanisms in the model in Scheme I. There are two plausible ways that crystal nucleation can occur in this system. The first is that during laser amorphization all crystallites are not eliminated, leaving what may be a substantial concentration of nucleation sites dispersed throughout the amorphous layer. A second extreme is that the laser pulse completely melts the amorphous layer. In this case, crystallization will proceed from the nucleation sites in the transition zone or from the semicrystalline base. Though the latter extreme is suggested by prior studies of the rate of polymer melting, it is possible that nucleation sites of high stability persist in the amorphized region.[18] Thus it is useful to consider the effects of such sites on the model developed in Scheme I.

If spherulitic growth were taking place throughout the amorphous region due to evenly distributed residual crystallites, one would expect to see behavior described by the Avrami equation for three-dimensional growth from a predetermined number of nuclei. In this case one would see the typical induction time and "s"-shaped curve indicative of spherulitic growth in the plots of the degree of recrystallization versus time. Examination of the data in Figure 4 shows no induction time or inflection point.

Another possibility is that both nucleation processes take place and the spherulitic growth is masked by growth from the interface. Modeling was done to see what nucleation density for spherulitic growth could be present and still be masked by the interfacial nucleation process. It was found that a nucleation density of greater than 1×10^9 cm^{-3} would be required to see an inflection point in the curve. At nucleation densities below this level the resultant bulk rate of transformation for spherulitic growth is considerably slower than that measured. Thus the observed zero-order growth process has already transformed the majority of the material before the time at which growth from any possible residual sites could compete with this process.

The second aspect of the model is that crystallization takes place in one dimension normal to the interface. If crystal growth were to be taking place in a three-dimensional spherulitic manner or propagating in a plane in two dimensions, one would again expect to see an induction time in the plots in Figure 4. Thus the lack of an induction time is consistent with crystallization proceeding in a one-dimensional or rodlike manner.

C. Secondary Crystallization. It is clear that the crystallization process in polymers can be complex. The process may not be a single event but rather it can be a collection of multiple interrelated processes. Historically, this multiplicity of events has been separated into primary and secondary crystallization processes where primary crystallization refers to the initial growth of crystallites and secondary crystallization refers to processes which further increase the degree of crystallinity within the boundaries of existing crystallites.[1] Alternatively, primary crystallization has sometimes been defined as the processes which take place from the initiation of a kinetic measurement until the time at which significant deviations take place from the Avrami model or other model of interest.[1,2] In this latter case secondary crystallization refers to all processes taking place after deviation from the model begins. For either situation, with these definitions, primary and secondary crystallization may themselves be a combination of multiple steps. Although there has been much speculation about these primary and secondary crystallization processes, there have been few direct observations about the nature of these events.

Vibrational spectroscopy has been used previously by Lin and Koenig and Bulkin et al. to observe multiple processes occurring upon crystallization of PET.[14,15] Lin and Koenig used IR spectroscopy to study the trans-

gauche isomerization of the ethylene glycol linkage in PET. Lin and Koenig observed a sigmoidal shape in their plots of the fraction of polymer in the trans state as a function of time. This behavior is consistent with that expected for bulk crystallization as described by the Avrami model. Following this primary step they also observed a secondary process which increases the trans content over a much longer period of time. Bulkin et al. using rapid-scanning Raman spectroscopy saw four distinct phases of crystallization in their plots of crystallinity as a function of time. They assign the four regions to an initial induction period for nucleation, a region of growth of small crystallites, an induction period due to the activation of chain disentanglement, and a final phase in which larger crystallites grow. In comparing their own data to that of Lin and Koenig, Bulkin et al. ascribe the secondary process observed by Lin and Koenig to an additional crystal perfection phase occurring after the four phases observed in ref 15.

As previously stated, in our data we do not observe an initial induction time in the crystallization process. In the present studies crystallization is initiated by nucleation sites present at the interface of laser-amorphized and semicrystalline PET. These sites are present immediately following the laser pulse which produces the amorphous region. In more traditional studies nucleation sites must form in the amorphous region. The time involved in the formation of these nuclei results in an induction time for the crystallization process. This also implies that unlike the situation we have described, with this latter mechanism there is not a single starting time for the entire crystallization process. In the present studies, the observed secondary process is compatible with a further increase in crystallinity within the boundaries of the semicrystalline material produced by primary crystallization. This secondary process may involve further conformational changes as a result of rotation about bonds within chains or chain packing within the framework generated by the primary process to produce a lower energy configuration. However, independent of the exact physical nature of the two processes, it is clear that the data we have obtained cannot be as well fit to a single simple functional form as to a combination of a zero-order and first-order kinetic transformation of the polymer. The transformations that are observed are compatible with a linear growth of the crystalline phase from a relatively sharp interface and subsequent first-order, secondary crystallization of this phase.

It should also be noted that in the time-resolved spectra reported here and in the depth-profiling spectra reported on in a separate publication, the intensities of absorptions associated with different functional groups of PET show different time dependencies on recrystallization. This also implies that recrystallization involves multiple processes since a single process would result in identical time dependencies for the various functional groups of the polymer. It is quite conceivable that some functional groups may be more sensitive to the change in environment associated with the primary process whereas other groups may show a greater change in local geometry due to secondary processes. Additionally, if secondary processes involve local transformations, then each functional group may have a different time dependence since each functional group is in principle subject to its own unique local potential.

The data also provide information on the first-order rate constants for the secondary crystallization process. These are reported in Table I. Interestingly, the temperature dependence of these rate constants follow a similar trend as the temperature dependence of k_1 which peaks at approximately 170 K. The maximum value of k_2 is also at approximately 170 K. This temperature dependence indicates that the secondary process cannot be modeled as a simple first-order process with a temperature-independent activation energy. An implication of this statement is that k_2 does not represent an elementary step but is rather a phenomenological description of multiple competing kinetic processes resulting in a temperature-dependent phenomenological rate constant which yields a maximum rate for the secondary process at a specific temperature.

V. Conclusions

The recrystallization of laser-amorphized PET films has been followed as a function of temperature using transient infrared spectroscopy. The time dependence of the fraction recrystallized has been obtained and is temperature dependent. This time dependence can be fit to a kinetic model involving a primary recrystallization step with crystallization proceeding at a constant rate perpendicular to the interface between the laser-amorphized and untreated material. This interface acts to nucleate the crystallization process. A secondary crystallization step, describable by first-order kinetics, further transforms the material that has undergone primary crystallization. The success of this treatment of the rate data indicates that if the elementary steps of crystallization can be isolated from one another, rates for these steps can be determined and a more detailed model for crystallization kinetics can be developed.

The rate of primary crystallization is seen to reach a maximum value of 94 nm/s at 170 °C, and the observed rates for primary crystallization are in good agreement with literature values for the spherulitic growth rate for PET of a similar molecular weight. These data then serve to indicate that laser amorphization does not degrade PET and thus confirm the thermal nature of the laser treatment process. Details of the microscopic nature of the primary and secondary crystallization processes have been discussed. The observation that the IR spectra of different functional groups respond differently to primary and secondary crystallization offers the possibility of an understanding of these processes at a level of the local geometry of the functional groups.

Acknowledgment. The work at Northwestern University was supported by 3M Corp. under their University Cooperative Research Program.

References and Notes

(1) *Polymer Handbook*, 3rd ed.; Brandrup, J., Immergut, E. H., Eds.; Wiley-Interscience: New York, 1989; p VI/279.
(2) *Encyclopedia of Polymer Science and Engineering*; Mark, H. F., Bikales, N. M., Overberger, C. G., Menges, G., Kroschwitz, J. I., Eds.; Wiley-Interscience: New York, 1989; p S 231.
(3) Van Krevelen, D. W.; Hoftyzer, P. J. *Properties of Polymers*; Elsevier: Amsterdam, 1976; Chapter 19.
(4) Wunderlich, B. *Macromolecular Physics. Crystal Nucleation, Growth, Annealing*; Academic: New York, 1976; Vol. 2.
(5) Dunn, D. S.; Ouderkirk, A. J. *Macromolecules* **1990**, *23*, 770.
(6) Stokr, J.; Schneider, B.; Doskocilova, D.; Lovy, J.; Sedlacek, P. *Polymer* **1982**, *23*, 714.
(7) Boerio, F. J.; Bahl, S. K.; McGraw, G. E. *J. Polym. Sci., Polym. Phys. Ed.* **1976**, *14*, 1029.
(8) McClure, D. J.; Ouderkirk, A. J.; Hill, J. B.; Dunn, D. S. *J. Vac. Sci. Technol., A* **1990**, *8* (3), 2295.
(9) Dunn, D. S.; McClure, D. J. *J. Vac. Sci. Technol., A* **1987**, *5* (4), 1327.
(10) Rabolt, J. F.; Jurich, M.; Swalen, J. D. *Appl. Spectrosc.* **1985**, *39* (2), 269.

(11) Van Antwerpen, F.; Van Krevelen, D. W. *J. Polym. Sci., Polym. Phys. Ed.* **1972**, *10*, 2423.
(12) Daubeny, R.; Bunn, C. W.; Brown, C. J. *Proc. R. Soc. London* **1954**, *226*, 531.
(13) Dunn, D. S.; Ouderkirk, A. J.; Richards, P. D.; Weitz, E., manuscript in preparation.
(14) Lin, S. B.; Koenig, J. L. *J. Polym. Sci., Polym. Phys. Ed.* **1983**, *21*, 2365.
(15) Bulkin, B. J.; Lewin, M.; McKelvy, M. L. *Spectrochim. Acta* **1985**, *41A*, 251.
(16) Demas, J. N. *Excited State Lifetime Measurements*; Academic: New York, 1983; p 83.
(17) Van Antwerpen, F.; Van Krevelen, D. W. *J. Polym. Sci., Polym. Phys. Ed.* **1972**, *10*, 2409.
(18) Ouderkirk, A. J.; Dunn, D. J., unpublished results.